XVII IAHR SYMPOSIUM
Beijing, China 1994

EVALUATION FROM MODEL TESTS FOR A PREDICTION OF THE STABILITY OF OPERATION OF FRANCIS TURBINES

Thierry JACOB and Jean-Eustache PRENAT, IMHEF - EPF Lausanne
Switzerland

ABSTRACT

This paper presents similitude laws for steady-oscillatory phenomena associated with the off-design operation of Francis turbines.
An appropriate procedure is proposed for stability of operation tests to be performed along with standard model tests.
The elaboration and presentation of oscillatory data is discussed.

RESUME

Cet article expose les conditions de similitude relatives aux phénomènes périodiques associés à l'exploitation des turbines Francis hors de leur domaine de fonctionnement optimal.
Une procédure est proposée pour la conduite d'essais de stabilité de fonctionnement à l'occasion des essais sur modèle réduit de turbines Francis.
L'élaboration et la présentation des résultats d'essais sont commentées.

L'article en français peut être obtenu auprès des auteurs.

G13

1. Introduction

Francis turbines may exceed 700 MW in unit power and 8 m in runner diameter. They often produce more than 100 MW with runners larger than 4 m. With these great dimensions and powers, it is quite impossible to test the machines before they are fully installed. As their efficiency and reliability hold a major role in the economic welfare of the whole project, technical guarantees for large turbines are most often checked on scale models in laboratory test installations [9].

Hydraulic fluctuations are a normal feature of Francis turbines operation [4, 6, 15, 21]. They originate in the interactions between rotating velocity fields and non-moving structures of the machine. They are influenced by the turbine hydraulic design, by operating conditions and by the dynamic response of the turbine hydraulic and electro-mechanical surroundings.

Low frequency fluctuations are basically the part load precession and the free oscillations of the water plug in the draft tube [12]. They may endanger the plant stability of operation if the penstock or generator response amplifies the excitation.

Similitude laws provide the conditions that must be achieved for the laboratory experiment (model test) to be homologous to the full-scale turbine (prototype) operation. Kinematic similitude laws are familiar to all hydro engineers. They ensure identical relative flow velocities in model and prototype. Dynamic similitude laws proceed from a more advanced analysis of forces acting on control volumes within the fluid.

Once similitude questions are settled, model tests provide a characterization of the dynamic behavior associated with a particular turbine design and a range of operation. Model tests are essential for a prediction of plant stability of operation. Model test results are mainly the types of observed disturbances, the excitation frequencies and magnitudes as well as the compliance of draft tube cavitation.

2. Similitude

2.1 Kinematic (flow) similitude

Kinematic similitude deals with the steady flow of an incompressible, non-viscous fluid through the turbine. Flow velocities in a small scale turbine model and in a geometrically similar full scale prototype are similar if all relevant velocity vectors at a reference point on the runner are similar. In practice, two velocity magnitudes are considered along with the head velocity $\sqrt{2\,E}$: the solid rotation U and the throughput velocity Cm at the runner outlet periphery ($_{Ie}$). Ratios of these magnitudes form the flow coefficient φ and energy coefficient ψ :

$$\varphi_{Ie} = \frac{Cm_{Ie}}{U_{Ie}} = \frac{Q}{\pi\, R_{Ie}^3\, \omega} \qquad \psi_{Ie} = \frac{\sqrt{2\,E}^{\,2}}{U_{Ie}^2} = \frac{2\,E}{R_{Ie}^2\, \omega^2} \tag{1}$$

2.2 Similitude laws resulting from the momentum equation

The momentum equation describes the balance of external (mass, pressure, friction) and internal (inertia) forces acting on a control volume within the flow:

$$\int_A \rho\, \vec{C}\, \vec{C}\cdot\vec{n}\, dA + \int_V \rho\, \frac{\partial \vec{C}}{\partial t}\, dV = \int_V \rho\, \vec{g}\, dV - \int_A p\, \vec{n}\, dA + \int_A \bar{\bar{\tau}} \cdot \vec{n}\, dA \tag{2}$$

Steady inertial forces	+ unsteady inertial forces	= mass (gravity) forces	- pressure forces	+ viscous forces

If X' and X" are corresponding parameters of the full-size and scale model systems, λ_X is the associated scale ratio: $X'' = \lambda_X \cdot X'$. Combinations of scale ratios must comply with some rules for the model test to be in similitude with the full-size machine operation.

Reynolds' similitude states that the ratio of steady inertia to viscous forces is the same on model and prototype. Satisfying both Reynolds and kinematic similitudes requires a full-scale experiment, so turbine model tests are never done at prototype Reynolds number. Efficiency discrepancies due to resulting scale effects are corrected using empirical step-up formulae.

$$\lambda_\rho \cdot \lambda_C^2 \cdot \lambda_L^2 = \lambda_\mu \cdot \lambda_C \cdot \lambda_L \quad \left(\lambda_\tau \text{ reduces to } \lambda_\mu \cdot (\lambda_C/\lambda_L)\right) \; ; \; Re = \frac{C \cdot L}{\mu/\rho} \tag{3}$$

Mach's and Euler's numbers both state that the ratio between steady inertia and pressure forces is the same on model and prototype. Euler's number is directly related to Thoma number σ, which states that local conditions for the appearance of cavitation are in similitude.

$$\lambda_\rho \cdot \lambda_C^2 \cdot \lambda_L^2 = \lambda_\rho \cdot \lambda_L^2 \qquad Ma = \frac{C}{\sqrt{dp/d\rho}} = \frac{C}{S} \; ; \; Eu = \frac{p - p_0}{\rho \cdot C^2} \; ; \; \sigma_{Ie} = \frac{NPSE_{Ie}}{E} \tag{4}$$

Froude's similitude states that the ratio between steady inertia and mass forces due to gravity is the same on model and prototype. Froude guarantees homology in pressure gradients due to gravity and to mean flow velocity. If both Thoma and Froude similitudes are achieved, then the similitude in local appearance of cavitation is extended to the whole flow domain [8].

$$\lambda_\rho \cdot \lambda_C^2 \cdot \lambda_L^2 = \lambda_\rho \cdot \lambda_g \cdot \lambda_L^3 \qquad Fr = \frac{C^2}{g \cdot L} \; ; \; Fr = \frac{2H}{R} \tag{5}$$

Strouhal's similitude states that the ratio between steady inertia and unsteady inertia forces is the same on model and prototype. Strouhal will provide the time basis for unsteady phenomena resulting from a given mean flow pattern.

$$\lambda_\rho \cdot \lambda_C^2 \cdot \lambda_L^2 = \lambda_\rho \cdot \lambda_C \cdot \lambda_t^{-1} \cdot \lambda_L^3 \qquad St = \frac{C \cdot \Delta t}{L} \tag{6}$$

2.3 Similitude of draft tube cavitation patterns and free oscillations

Under the joint action of a low energy level and of high peripheral velocities in the runner exit swirling flow, local pressures drop to vapor pressure and a cavity forms within the draft tube flow. The elastic effect of this vapor volume V_v influences the free oscillations of the water plug in the draft tube. In a discrete two-elements model, the frequency of free oscillations is determined by the compliance $\tilde{C}$ of draft tube cavitation and by the inertia $\tilde{L}$ of the water plug in the draft tube. If the draft tube outlet opens on a large vessel or a free water level, then:

$$f_0 = \frac{1}{2\pi}\left(\tilde{C}\,\tilde{L}\right)^{-1/2}, \text{ with } \quad \tilde{C} = -\frac{\partial V_v}{\partial NPSE} \quad \text{and} \quad \tilde{L} = \int \frac{dl}{A} \tag{7}$$

Is the cavity volume similar on model and prototype? Theoretically, Thoma, Froude and flow similitudes should be obeyed to ensure analog conditions for cavitation over the whole vertical extent of the cavity. Froude similitude, however, is not easily fulfilled. Associated with flow similitudes, Froude requires the head and dimensions scales to be equal: $\lambda_H = \lambda_R$. High power turbines for low heads have large dimensions, and the models have a very small dimensional scale; Froude head is then so low that test conditions would be very bad. High head turbines, on the other hand, are seldom very large. As the model can't be too small, Froude head may then reach very high values, leading to excessive model test power and mechanical stresses.
Few references give comparisons of draft tube cavity patterns in model and prototype. The existing evidence [4] suggests that relative dimensions are the same if flow and cavitation are in similitude. In that case, the scale ratio on the frequency of free oscillation is the same as for the rotational frequency:

$$\lambda_{f0} = \left(\lambda_{\tilde{C}}\,\lambda_{\tilde{L}}\right)^{-1/2} = \left(\lambda_R^3 \cdot \lambda_\sigma^{-1} \cdot \lambda_E^{-1} \cdot \lambda_R^{-1}\right)^{-1/2} = \lambda_E^{1/2} \cdot \lambda_R^{-1} = \lambda_n \quad \text{as} \quad \lambda_\sigma = \lambda_\psi = 1 \tag{8}$$

Failure to comply with Froude similitude introduces an influence of the reference elevation for NPSE in Thoma similitude. An ill-chosen reference will change cavitation conditions according to the turbine size and head. Extensive laboratory testing [14] showed that there is no noticeable influence of the test head on the relative frequency of free oscillation and on the observable cavity volumes if the reference elevation is set at the runner outlet periphery: $\sigma = \sigma_{Ie}$.

2.4. Similitude of disturbance frequencies

Strouhal's similitude involves a flow velocity, a reference length and a time basis. Combined with either energy or flow coefficients, this shows that the frequency of disturbances associated with the mean velocity distribution and the rotational frequency have the same scale ratio:

$$\begin{cases} \lambda_f = \lambda_C \cdot \lambda_L^{-1} = \lambda_E^{1/2} \cdot \lambda_R^{-1} = \lambda_n \quad \text{as} \quad \lambda_\psi = 1 \\ \lambda_f = \lambda_C \cdot \lambda_L^{-1} = \lambda_Q \cdot \lambda_R^{-3} = \lambda_n \quad \text{as} \quad \lambda_\varphi = 1 \end{cases} \tag{9}$$

This general similitude is in agreement with the frequency parameter (fD^3/Q or other) [18, 21] definitions for vortex-generating devices with non-rotating vanes. It is valid for most of the flow instabilities due to turbine off-design operation. Disturbances due to viscous effects must be handled more cautiously, since Reynolds similitude is never achieved.

2.5 Similitude of disturbance amplitudes

The amplitude of pressure fluctuations is related to variations of flow velocity through the pressure and unsteady inertia forces in the momentum equation:

$$\lambda_p \cdot \lambda_C \cdot \lambda_t^{-1} \cdot \lambda_L^3 = \lambda_{\Delta p} \cdot \lambda_L^2 \quad ; \quad \lambda_{\Delta p} = \lambda_p \cdot \lambda_C \cdot \lambda_L \cdot \lambda_t^{-1} \tag{10}$$

The reference dimension is the runner radius; the runner rotation provides the time basis. The reference velocity is derived from the energy coefficient: $\lambda_C = \lambda_E^{1/2} = \lambda_R \cdot \lambda_n$ as $\lambda_\psi = 1$

$$\lambda_{\Delta p} = \lambda_p \cdot \lambda_C \cdot \lambda_R \cdot \lambda_n = \lambda_p \cdot \lambda_E^{1/2} \cdot \lambda_R \cdot \lambda_n = \lambda_p \cdot \lambda_E \tag{11}$$

This shows that the amplitude of pressure oscillations has the same scale ratio as the pressure associated with the turbine specific hydraulic energy. This general similitude is in agreement with the amplitude parameter ($D^4\Delta p/\rho Q^2$ or other) definitions for vortex-generating devices with stationary vanes [18, 21]. Of course, this is true only at the emission of disturbances. Pressure waves propagate in the piping system, are reflected, and the observed amplitudes are strongly influenced by standing waves. That's why the similitude of pressure amplitudes is lost in case of dynamic interaction with the hydraulic circuit.

2.6 Similitude of acoustic power emission, prediction of prototype amplitudes

The global acoustic power GAP is the active power associated with a hydraulic oscillation [1, 3, 7, 13, 20]. It combines pressure and kinetic energies. It is not influenced by standing waves in the piping: GAP(x,f) = GAP(f). More basically, it is equal to the difference between squared forward and backward travelling pressure waves magnitudes, divided by the reference acoustic impedance $Z_0 = \rho S/A$. If it is again multiplied by the reference impedance, it reduces to a balance of squared pressure disturbances, which may be transposed using their ratio to the turbine specific hydraulic energy E (equation 11) [13].

$$GAP(f) = \text{Real}\left(p(x,f) \cdot q^*(x,f) \right) \quad ; \quad \lambda_{GAP} = \lambda_{\Delta p} \cdot \lambda_{\Delta Q} = \lambda_{\Delta p}^2 \cdot \lambda_{Z0}^{-1} = \lambda_p^2 \cdot \lambda_E^2 \cdot \lambda_{Z0}^{-1} \tag{12}$$

The transmission of acoustic waves through the turbine is linear up to high amplitude levels [15], so the active part of the oscillation propagates from the region of emission (in the draft tube) to the spiral case inlet (where the global acoustic power may be evaluated) without being corrupted by superimposed standing waves from the test circuit.

It may be difficult to make a good measurement of acoustic power emission if the ratio of travelling to standing waves is too low (that is, if the phase of the spiral case inlet hydraulic impedance is too close to $\pm \pi/2$) [20].

The global acoustic power, transposed from model test data to the prototype dimensions and operating conditions, may be combined with the hydraulic impedance from the prototype penstock to compute the magnitude of pressure oscillations at the spiral case inlet. This predicted pressure oscillation magnitude is compatible both with the disturbances generated by the turbine operation and with the standing waves resulting from the plant layout [15].

3. Evaluation of turbine stability of operation from model tests

3.1 Test arrangement and expected results

An investigation of stability of operation should be included in all model testing of Francis turbines. It takes typically one or two days, depending on the desired amount of data. The test results give a clear overall representation of steady-oscillatory phenomena. Their main contents are:

- for the oscillation associated with the part-load precession: frequency, pressure amplitudes in two positions across the draft tube cone and at the spiral case inlet, phase shift of pressure signals across the draft tube cone; occasionally, information on the second harmonic;
- for the free oscillations of the water plug in the draft tube against the elastic vapor volume due to draft tube cavitation: frequency (there may be several frequencies at full load), pressure amplitudes at full load, occasionally pressure amplitudes at part load.
- observations of draft tube cavitation with comments.

Considering the elements of similitude commented in section 2 of this paper, these test results characterize the considered turbine design and operating conditions. They provide the basis for a prediction of the stability of operation of the full-size turbine.

Dynamic behaviors associated with turbine designs and operating conditions may be compared in the scope of competitive model tests, or with model data from the existing turbine in the case of upgrade projects [9]. The prediction of stability of operation, however, requires an impedance analysis of the full-size turbine layout, including penstock, manifold, gate shafts etc [15].

3.2 Test conditions

The test hydraulic specific energy is chosen so that oscillation amplitudes and frequencies fall within favorable ranges of the instruments. When Froude head is beyond the possibilities of the model or instruments, a more adequate test head is chosen. Care must then be taken in setting the reference elevation for Thoma number σ at the runner outlet periphery ($\sigma_{\overline{1e}}$), see § 2.3.

Minimum testing is a variation of guide vane opening at the main plant energy number under a constant test head, at plant σ. Typically twenty test points are spread from 50% of best efficiency flow, where part load rotation isn't quite organized, up to the prototype maximum gate opening, and a little bit beyond that if possible. Detailed testing at part load (about 60% of φ_{opt}) and at full load (about 120% of φ_{opt}) give a fair idea of oscillatory phenomena with slightly different operating conditions. These consist in one variation of model rotational speed with constant test head and σ, one variation of σ and possibly a variation of test head.

This amount of data is absolutely necessary for an appropriate diagnosis of the turbine dynamic behavior [12]. The data from the test points selected for cavitation observations or efficiency weighting alone doesn't allow a proper perception of dynamic phenomena.

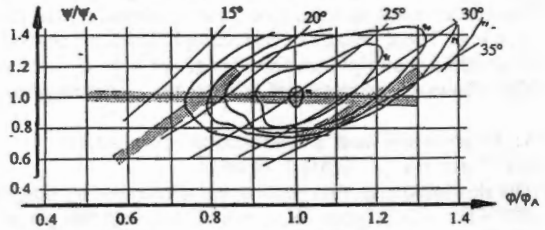

figure 1: Francis turbine stability of operation test paths

As plant σ depends strongly on the particular conditions of the project, the basic test should be repeated at the reference σ, $\sigma_{ref} = 0.2/\psi_{\overline{1e}}$ [17], which allows comparison between machines of different designs and specific speeds. For projects with large variations of head, partial tests should also be performed for different energy coefficients, with corresponding σ values.

3.3 Instrumentation

Pressure fluctuations are measured using highly sensitive transducers with a suitable dynamic response. The sensors are flush mounted on the turbine model walls. If this can't be done, dynamic influences of the connecting pipes must be evaluated and compensated for in the

processing of results. For common testing, the pressure sensors frequency band goes at least from one eighth to three times the turbine model rotational frequency. Their sensitivity must allow the detection of fluctuations with a root mean square amplitude equal to 0.1% of the test head pressure, with a minimum threshold of 0.1 to 0.2 mbar. The signal conditioning electronics must not introduce phase shifts between the various signals.

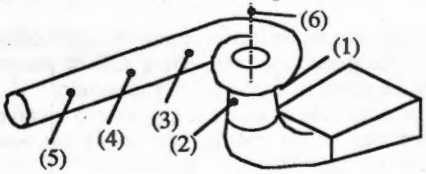

figure 2: Schematic view of pressure sensors

The tested model is equipped with:

- one pressure sensor on the draft tube cone wall, close to the runner outlet, in the turbine main axis, on the draft tube outlet side: "downstream cone" (1);
- one pressure sensor on the draft tube cone wall, close to the runner outlet, in the turbine main axis, on the opposite side: "upstream cone" (2);
- one pressure sensor on the feed pipe wall, at spiral case inlet: "spiral case inlet" (3);
- if possible, two additional pressure sensors on the feed pipe walls, forming two equal lengths of uniform pipe for acoustic power analysis (4), (5)
- if possible, a torque sensor on the turbine shaft (6)
- according to possibilities, additional pressure sensors on the draft tube wall.

Amplifier output signals are low-pass filtered to remove high frequency noise and sampled so as to preserve the phase shift information. The sampling rate is high enough to minimize aliasing effects. Processing is done over at least 400 runner revolutions.
Draft tube cavitation is observed and schematically drawn for each test point.

3.4 Particular requirements for pressure fluctuations tests

All wet parts of the model (except seals) must be geometrically similar to those of the prototype. The model construction must be stiff enough to prevent excessive deformations.
Transparent parts on the low pressure side of the runner must be large enough for observation of cavitation not only on the runner blades, but also in the upper portion of the draft tube.
The draft tube outlet opens in a tank with a surface large enough to ensure the dynamical uncoupling of the low pressure part of the test circuit. The feed pipe free oscillations frequency must be lower than one eighth of the model rotational frequency or higher than three times that frequency in order to avoid undesirable resonance of the test circuit. Hydraulic disturbances from the feed pump should not be felt at the model in this range of frequencies.
The test installation should operates in closed circuit mode, so the dissolved gas content can be kept low. There mustn't be travelling bubbles at the model inlet.
If possible, a straight uniform length of pipe is fitted on the high pressure side of the model. This allows an estimation of acoustic waves propagation conditions at the spiral case inlet.

4. Processing and presentation of results

4.1 Note on presented results

The discussions in this section are illustrated by diagrams from the model tests conducted at IMHEF for BC Hydro's Kootenay Canal upgrade project. The Kootenay River lies in southern British Columbia, Canada. The four units are 5 m in runner diameter. They operate under a maximum head of 81 mWC. Increases in unit power often raise problems in stability of operation. Upgrade projects are specially interesting: they allow the comparison of the dynamic behavior of proposed new turbine designs with the known behavior of the existing turbine.

4.2 Preliminary processing [16]

Hydraulic fluctuations associated with Francis turbines operation occur at various frequencies, not multiples of the rotational frequency. The different frequency components of signals must be tracked across variations of operation parameters. That's why recordings are systematically

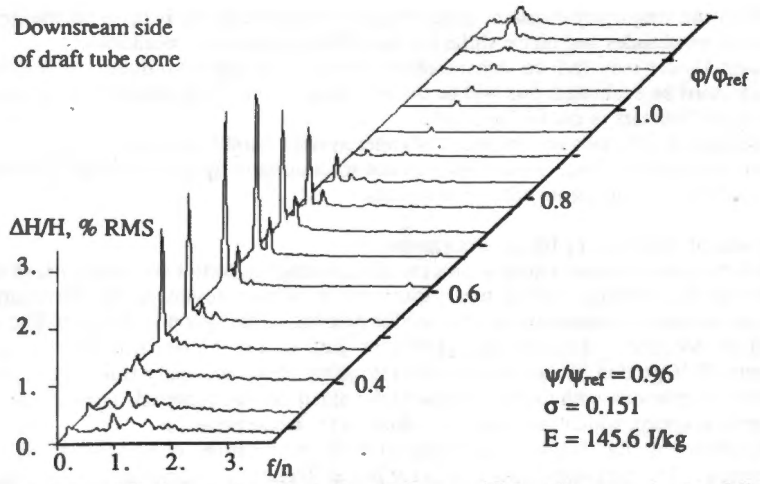

figure 3: Waterfall diagram for a variation of flow coefficient from part load to full load

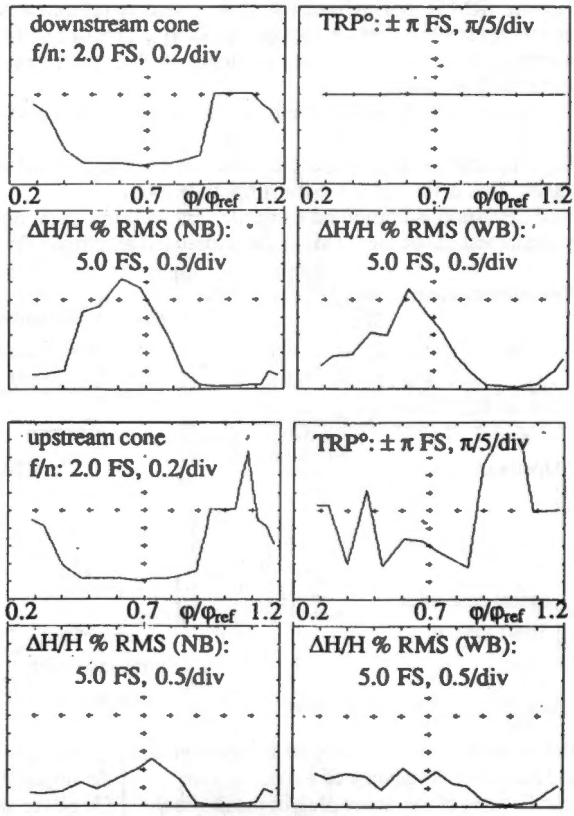

figure 4: Summarized diagrams at downstream and upstream sides of draft tube cone for a variation of flow coefficient from part load to full load at 0.96 ψ_{ref}, $\sigma = 0.151$, E = 145.6 J/kg

analyzed in the frequency domain. Interpretation of observations is done on the grounds of frequencies, amplitudes and phase shifts for the different operating conditions.
The circuit layout may induce considerable distortion in the amplitudes. If the excitation magnitude must be evaluated, this will be done by acoustic analysis using the signals from three equally spaced sensors in the feed pipe [13].
Only sustained oscillations are liable to endanger system stability of operation. Isolated shocks and bursts and random fluid-borne noise are not so important. Spectral averaging enhances the steady-oscillatory components of the test signals.

4.3 Standard oscillatory data diagrams

The oscillatory data is automatically processed to produce waterfall and summarized diagrams of hydraulic fluctuations versus test parameter. It is then reviewed by the operator and significant spectral components are selected for plotting in the synoptic diagram. The selection is based on frequency-domain magnitudes as well as on inter-channel phase shifts and coherences. It is guided by an overall understanding of the unsteady flow in the draft tube. Oscillatory phenomena with unclear physics are sometimes encountered. They can be added to the synoptic diagram, which may later contribute to their interpretation.
Waterfall diagrams (fig. 3) give three-dimensional representations of pressure oscillations amplitude spectra. The horizontal axis stands for linear frequency, normalized by the runner rotational frequency. The vertical axis stands for pressure oscillation or shaft torque linear amplitude, root mean square (RMS), normalized by the test head or reference torque. The diagonal axis stands for the test parameter: flow or energy coefficient, Thoma number or test head.
Summarized diagrams (figure 4) retain the frequency with the greatest amplitude for each measurement channel and test point.
The frequency is normalized by the runner rotational frequency and plotted versus test parameter.
The corresponding amplitude from the spectral data is normalized by the test head and plotted versus test parameter. This is the narrow-band amplitude (NB).
The signal standard deviation is computed from the sampled time data, normalized by the test head and plotted versus test parameter. This is the wide-band amplitude (WB).

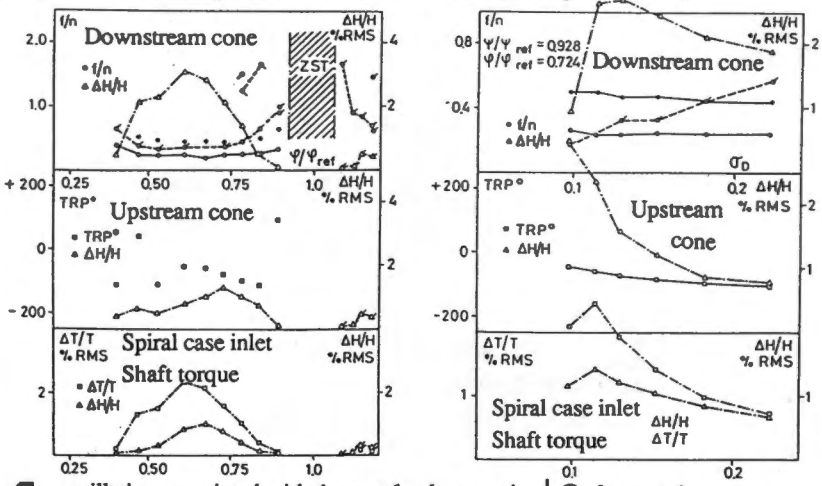

○, △, □	oscillation associated with the part-load precession	○: frequencies
●	second harmonic frequency of the precession	△: amplitudes
♂, ♂	free oscillations of the water plug in the draft tube	□: phase shifts(ref.downstream side of cone)
♀, ♀	high partial load oscillation frequencies	

figure 5: Synoptic diagram with vortex-free region (ZST). See fig. 6 for operating conditions.

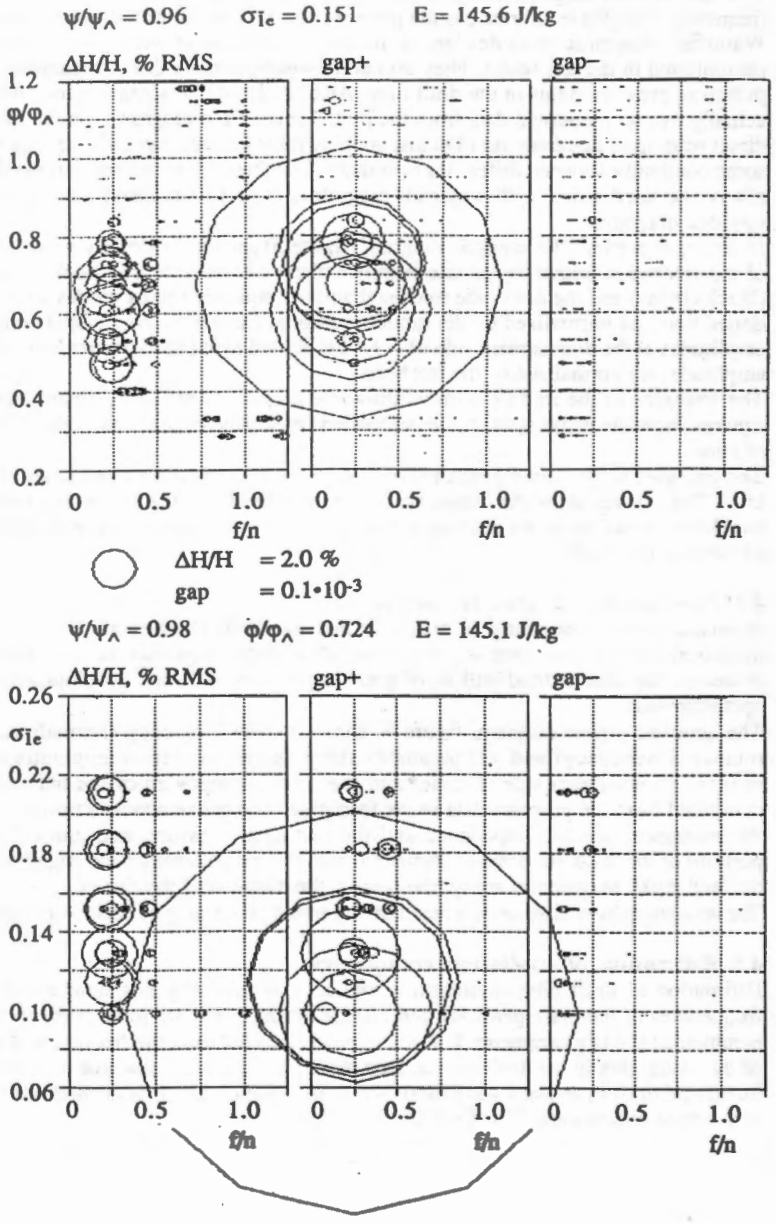

figure 6: Acoustic power diagrams for operating conditions of figure 4.

Comparison of NB and WB amplitude gives an indication as to whether harmonics, non-synchronous peaks or wide-band noise add to the dominant sine component of the signal.
The summarized diagram also provides the phase of the considered channel at the dominant frequency. The phase reference is the pressure signal from the downstream side of cone.
Waterfall diagrams provides an immediate overview of steady-oscillatory phenomena encountered in the test series. They do not, however, allow a direct separation of rotating and pulsating pressure fields in the draft tube. Also, their 3-D presentation may make it painful to actually extract numerical data from the plot. Summarized diagrams, on the other hand, give a direct reading of dominant oscillations, but they must be used carefully, as they tend to construe some continuity between different phenomena. For these reasons, summarized diagrams should always be used along with waterfall diagrams. A more advanced analysis is based on the synoptic diagram.
In its upper portion, the synoptic diagram (figure 5) shows the evolution versus test parameter of the precession frequency (in this example, blank circles with solid line), its second harmonic (black circles) and the draft tube free oscillations frequency (blank circles with upward tail and dotted line), all normalized by the runner rotational frequency. Associated pressure oscillation amplitudes at the downstream side of cone are plotted using triangles with the same styles. The amplitudes are normalized by the test head.
The triangles in the middle portion show the amplitude at the upstream side of cone. The squares show the phase shift, at the precession frequency, of upstream side to downstream side of cone.
The triangles in the lower portion show the pressure oscillation amplitudes at the spiral case inlet. The squares show the torque oscillation amplitudes at the precession frequency. Torque oscillation amplitudes are normalized by the reference torque (best efficiency torque at the considered test head).

4.4 Presentation of acoustic power data

Acoustic power processing is presently not standard. Queries as to the precision of this measurement still need clear answers based on in-depth experimentation. There is little doubt, however, that this method will be of great importance in future developments of stability of operation tests.
The acoustic power diagram, figure 6, shows versus frequency (normalized by the runner rotational frequency) and test parameter the pressure oscillation amplitude at the reference channel (downstream side of cone) and the active component of the hydro-acoustic power computed from the pressure data in the feed pipe. The active acoustic power is normalized by the reference acoustic impedance and the test head pressure, and plotted in two separate portions of the diagram: positive (radiating from the model turbine) and negative (radiating from the feed pipe). Magnitudes are symbolized by the diameter of the circles.
The acoustic power diagram is a result of automatic processing of oscillatory data.

4.5 Estimation of cavitation compliance

Estimation of draft tube cavitation compliance is presently not standard. If the resonance frequencies of the plant penstock and turbine arrangement are to be computed, the cavitation compliance is a key parameter. It is conveniently derived from the frequency of free oscillations of the water plug in the draft tube against the elastic vapor volume due to cavitation, using the integrated draft tube water plug inertance as in equation (7). It is normalized by the test head and turbine dimensions: $\bar{C}^* = \bar{C} \cdot E/R^3$.

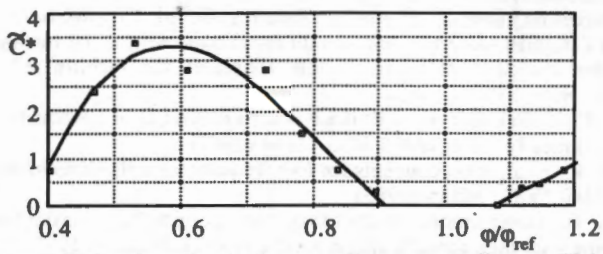

figure 7: Estimation of cavitation compliance versus flow coefficient

5. Conclusions

A detailed analysis of scale relations between forces in the momentum equation was performed. Combined with elements of kinematic (flow) similitude, these scale relations lead to similitude rules for the study of steady-oscillatory problems associated with Francis turbine operation in off-design conditions. These similitude rules are in agreement with the experience gained over years of laboratory testing and with the available model to prototype comparisons.

A model test procedure based on these elements of similitude allows a quick and complete description of the turbine behavior in steady-oscillatory conditions. The test results are representative of the turbine hydraulic design and operating conditions. A large part of the processing is done automatically.

Appropriate diagrams clearly show the particular oscillatory features of the considered turbine design.

The authors thank BC Hydro for permitting the publication of test results.

Symbols

A	Cross-sectional area	m^2
Cm	Throughput velocity	m/s
D	Diameter	m
Eu	Euler number	
f_0	Frequency of free oscillations	Hz
g	Gravity	m/s^2
gap	Non-dimensional acoustic power	
l	Element length	m
$\bar{L}$	Inertance	m^{-1}
n	Rotational frequency ($n = \omega/2\pi$)	Hz
NPSE	Net positive suction energy	J/kg
q	Frequency volume flow-rate	m^3/s
R	Runner reference radius (at $_{fe}$)	m
S	Wave propagation speed	m/s
t	Time	s
V	Volume	m^3
X	Parameter	
φ	Flow coefficient	
Δ	Difference, variation, amplitude	
μ	Dynamic viscosity	$m^5\ kg^{-1}\ s^{-1}$
ρ	Mass per unit volume	kg/m^3
ω	Runner angular speed	rad/s
$_0$	(subscript) Reference	
$_{fe}$	(subscript) Runner blade outlet periphery	
$_{opt}$	(subscript) Optimal operating conditions	

C	Reference or flow velocity	m/s
$\bar{C}$	Compliance	$m\ s^2$
E	Specific hydraulic energy	J/kg
f	Frequency	Hz
Fr	Froude number	
GAP	Global acoustic power	W
H	Head (height of liquid column)	m
L	Length	m
Ma	Mach number	
$\vec{n}$	Normal vector	
p	Time or frequency pressure	N/m^2
Q	Time volume flow-rate	m^3/s
Re	Reynolds number	
St	Strouhal number	
U	Peripheral (solid) velocity	m/s
x	Abscissa	m
Z_0	Reference impedance	$m^{-1}\ s^{-1}$
ψ	Energy coefficient	
λ_X	Scale ratio for parameter X	
σ	Thoma number	
$\bar{\bar{\tau}}$	Stress tensor	N/m^2
$_{ref}$	(sub) Reference operating conditions	
$_v$	(subscript) Vapor	
*	(superscript) Complex conjugate	

References

[1] BADIE-CASSAGNET A. et al.: Application de l'intensimétrie acoustique à l'identification des sources de pulsation de pression dans les circuits. CETIM, Senlis (1981)

[2] CAMPMAS P., GIRAUD H.: Analyse du fonctionnement d'une turbine Francis: comparaison des investigations sur modèle réduit et sur turbine industrielle. AIRH Symposium, Nice (1960)

[3] DESMET B., TEPHANY F., TROLLE J.L., OUAKED R.: Acoustic power method applied to a butterfly valve. IAHR W.G., Lille (1987)

[4] DÖRFLER P.: Evaluation concepts for low frequency oscillations in hydraulic reaction turbines. IAHR W.G., Milan (1983)

[5] DÖRFLER P.: Observations of draft tube pulsations at high partial load on a Francis model turbine with high specific speed. IAHR W.G., Lausanne (1993)

[6] FISHER R.K., ULITH P.: Comparison of draft tube surging of homologous scale models and prototype Francis turbines. Voith Research and Construction vol 28e (1982)

[7] GARREAU D., LEDUCQ B., TROLLE J.L.: Analyse expérimentale des phénomènes d'interaction d'une machine et de son circuit. Société Hydrotechnique de France (1987)

[8] HENRY P.: La cavitation dans les machines hydrauliques. Publication EPFL, Lausanne (1984)

[9] HENRY P., MOMBELLI H.P.: Hydraulic machinery model testing, IMHEF test facilities. Waterpower '93, Nashville(1993)

[10] HOSOI Y.: Contributions to model tests of draft tube surges of Francis turbines. IAHR Symposium, Fort Collins (1978)

[11] JACOB T., MARIA D., PRENAT J.-E.: Comportement dynamique d'une turbine Francis à forte charge. Comparaisons modèle - prototype. SHF Comité technique 134, Paris (1987)

[12] JACOB T., PRENAT J.E., GRENIER R.: A characterization procedure for the dynamic behavior of Francis turbines: Practical comparison of elbow and Moody type draft tubes. IAHR Symposium, Trondheim (1988)

[13] JACOB T., PRENAT J.E.: Generation of hydro-acoustic disturbances by a Francis turbine model and dynamic behavior analysis. IAHR Symposium, Belgrade (1990)

[14] JACOB T., PRENAT J.E., VULLIOUD G., LOPEZ ARAGUAS B.: Surging of a 140 MW Francis turbine at high load, analysis and solution. IAHR Symposium, São Paulo (1992)

[15] JACOB T.: Evaluation sur modèle réduit et prédiction de la stabilité de fonctionnement des turbines Francis. Thèse No 1146, EPFL, Lausanne (1993)

[16] JACOB T., PRENAT J.E.: Model testing for the stability of operation of Francis turbines. MTM Conference, Budapest (1994)

[17] KERCAN V., BAJD M.: Computation and experimental investigation of draft tube vortex in Francis turbines of various specific speed. IAHR Symposium, Trondheim (1988)

[18] NISHI M., MATSUNAGA S., KUBOTA T., SENOO Y.: Surging characteristics of conical and elbow-type draft tubes. IAHR Symposium, Stirling (1984)

[19] NISHI M., OKAMOTO M., WANG X.: Evaluation of pressure fluctuations caused by cavitated spiral vortex core in the swirling flow of elbow draft tube. IAHR W.G., Lausanne (1993)

[20] OUAKED R.: Etude des phénomènes propagatifs en conduite dans un circuit hydraulique: intensimétrie hydroacoustique. Thèse 400, USTL Flandres-Artois (1989)

[21] PALDE U.: Model and prototype turbine draft tube surge analysis by the swirl momentum method. IAHR Symposium, Vienna (1974)

[22] WEGNER M.: Cavitation as erosion and instability cause - experiments and remedies. Lahore (1983)